Cellular and Molecular Mechanisms of Atrial Arrhythmogenesis in Patients with Paroxysmal Atrial Fibrillation

Niels Voigt, MD[#,1,2], **Jordi Heijman, PhD**[#,1], **Qiongling Wang, PhD**[3], **David Y. Chiang, BSc**[3], **Na Li, PhD**[3], **Matthias Karck, MD**[4], **Xander H.T. Wehrens, MD, PhD**[3], **Stanley Nattel, MD**[5], and **Dobromir Dobrev, MD**[1,2]

[1]Institute of Pharmacology, Faculty of Medicine, University Duisburg-Essen, Essen, Germany

[2]Division of Experimental Cardiology, Medical Faculty Mannheim, Heidelberg University, Mannheim, Germany

[3]Cardiovascular Research Institute, Department of Molecular Physiology and Biophysics and Department of Medicine, Baylor College of Medicine, Houston, USA

[4]Department of Cardiac Surgery, Heidelberg University, Heidelberg, Germany

[5]Department of Medicine, Montreal Heart Institute and Université de Montréal and Department of Pharmacology and Therapeutics, McGill University, Montreal, Canada

[#] These authors contributed equally to this work.

Abstract

Background—Electrical, structural and Ca^{2+}-handling remodeling contribute to the perpetuation/progression of atrial fibrillation (AF). Recent evidence has suggested a role for spontaneous sarcoplasmic-reticulum Ca^{2+}-release events (SCaEs) in longstanding persistent AF, but the occurrence and mechanisms of SCaEs in paroxysmal AF (pAF) are unknown.

Method and Results—Right-atrial appendages from control sinus-rhythm patients (Ctl) or patients with pAF (last episode median 10-20 days preoperatively) were analyzed with simultaneous measurements of $[Ca^{2+}]_i$ (Fluo-3) and membrane-currents/action potentials (patch-clamp) in isolated atrial cardiomyocytes, as well as Western blot. Action potential duration, L-type Ca^{2+}-current and Na^+/Ca^{2+}-exchange current were unaltered in pAF, indicating absence of AF-induced electrical remodeling. In contrast, there was an increased incidence of delayed afterdepolarizations (DADs) in pAF. Ca^{2+}-transient (CaT)-amplitude and sarcoplasmic-reticulum Ca^{2+}-load (caffeine-induced CaT-amplitude, integrated membrane current) were larger in pAF. CaT-decay was faster in pAF but decay of caffeine-induced CaT was unaltered, suggesting increased Serca2a function. In agreement, phosphorylation (inactivation) of the Serca2a-inhibitor protein phospholamban was increased in pAF. Ryanodine-receptor (RyR2) fractional phosphorylation was unaltered in pAF, whereas RyR2-expression and single-channel open probability were increased. A novel computational model of the human atrial cardiomyocyte

Corresponding Author: Dobromir Dobrev, Hufelandstrasse 55, 45122 Essen; Phone: 0049-201-723-3477, Fax: 0049-201-723-5593; Dobromir.Dobrev@uk-essen.de.

indicated that both RyR2 dysregulation and enhanced Serca2a activity promote increased sarcoplasmic-reticulum Ca^{2+}-leak and SCaEs, causing DADs/triggered activity in pAF.

Conclusions—Increased diastolic sarcoplasmic-reticulum Ca^{2+}-leak and related DADs/triggered activity promote cellular arrhythmogenesis in pAF-patients. Biochemical, functional and modeling studies point to a combination of increased sarcoplasmic-reticulum Ca^{2+}-load related to phospholamban-hyperphosphorylation and RyR2 dysregulation as underlying mechanisms.

Keywords

paroxysmal atrial fibrillation; calcium handling; calcium leak; remodeling; computational modeling

Introduction

Atrial fibrillation (AF) is the most common arrhythmia in clinical practice, with an incidence that is rising with aging of the population.[1] AF is associated with increased morbidity and mortality, particularly due to embolic stroke and worsening heart failure.[1] Currently, AF is classified based on its clinical presentation: patients often first show paroxysmal AF (pAF), consisting of self-terminating episodes lasting <7 days, then persistent and finally long-lasting persistent (chronic) states (cAF) that fail to self-terminate.[2] Up to 15% of pAF-patients progress to persistent forms annually,[3] likely because of AF-related remodeling. The type of AF also affects clinical outcome, with cAF associated with worse outcomes and less amenable to rhythm-control therapy than pAF.[4]

The cellular and molecular mechanisms contributing to atrial arrhythmogenesis in cAF have been studied extensively with atrial-tissue samples from cAF-patients.[5-8] Combined with results from animal models,[9-11] these studies have highlighted a complex pattern of electrical, structural and Ca^{2+}-handling remodeling, producing a vulnerable substrate for AF-maintenance. However, the cellular mechanisms underlying pAF remain elusive.

Clinical AF initiates when triggers act on arrhythmogenic substrates. The pulmonary veins (PVs) play a particularly-important role in pAF-patients;[12] and there is evidence that PV-cardiomyocytes possess properties predisposing to both Ca^{2+}-driven focal activity and reentry.[2] Although atrial myocytes from pAF-patients undergoing open-heart surgery represent a potentially-useful model to study the basic mechanisms underlying AF-triggers, studies of the cellular electrophysiological changes that predispose to AF-paroxysms in patients are very limited.[13, 14]

The present study tested the hypothesis that patients with pAF are predisposed to Ca^{2+}-driven delayed afterdepolarizations (DADs), and studied potential underlying mechanisms with the use of simultaneous measurements of intracellular $[Ca^{2+}]$ ($[Ca^{2+}]_i$) and membrane-currents or action potentials (APs, patch-clamp), biochemical analyses, studies of ryanodine-receptors (RyR2) in lipid-bilayers and computational modeling.

Methods

A detailed description of all methods is provided in the online-only supplement.

Human Tissue Samples and Myocyte Isolation

Right-atrial appendages were dissected from 73 sinus-rhythm (Ctl) patients and 47 pAF-patients undergoing open-heart surgery. pAF-patients had at least one documented AF-episode that self-terminated within 7-days of onset (for one example, see Online Figure I). Patient characteristics are provided in Online Tables I-III. AF-characteristics were determined based on clinical information in the chart; the last AF-episode had terminated a median of 10-20 (range 1-72) days pre-operatively and all patients were in sinus-rhythm at the time of surgery. No detailed information was available regarding frequency and duration of AF-episodes. Experimental protocols were approved by the Medical Faculty Mannheim, Heidelberg University (No. 2011–216N-MA). Each patient gave written informed consent. After excision, atrial appendages were flash-frozen in liquid-N_2 for biochemical/biophysical studies or were used for myocyte isolation with a previously-described protocol.[15, 16] Isolated cardiomyocytes were suspended in EGTA-free storage solution until simultaneous measurement of intracellular Ca^{2+} ($[Ca^{2+}]_i$) and membrane current/potential.

Simultaneous Intracellular-Ca^{2+} and Patch-clamp Recording

$[Ca^{2+}]_i$ was quantified with Fluo-3-acetoxymethyl (Fluo-3) ester in bath and pipette solution. After de-esterification, fluorescence was excited at 488 nm and emitted light (>520 nm) converted to $[Ca^{2+}]_i$ assuming

$$\left[Ca^{2+} \right]_i = k_d \left(\frac{F}{F_{max} - F} \right)$$

where k_d is the dissociation constant of Fluo-3 (864 nmol/L), F=Fluo-3 fluorescence, and F_{max} is Ca^{2+}-saturated fluorescence obtained at the end of each experiment.[17]

Membrane-currents and APs were recorded at 37°C in whole-cell ruptured-patch configuration using voltage/current-clamp techniques with simultaneous $[Ca^{2+}]_i$ measurement. There was no significant difference in membrane capacitance between pAF (102.0±11.7 pF, n=15/9 [myocytes/patients]) and Ctl (113.6±6.1 pF, n=35/25; *P*=0.340) myocytes. Currents are expressed as current-densities (pA/pF). L-type Ca^{2+}-current ($I_{Ca,L}$)-triggered $[Ca^{2+}]_i$-transients were recorded simultaneously, as previously described.[15] Sarcoplasmic-reticulum (SR) Ca^{2+}-leak was measured as the decrease in $[Ca^{2+}]_i$ following application of tetracaine in the absence of extracellular Ca^{2+}/Na^+, as described by Shannon et al.[18]

Biochemistry

Protein-expression of calmodulin, calsequestrin-2, Ca^{2+}/calmodulin-dependent protein-kinase-II (CaMKII), GAPDH, Na^+/Ca^{2+}-exchanger (NCX1), phospholamban (PLB), catalytic and regulatory protein kinase-A (PKA) subunits, protein phosphatase type-1 and type-2A, ryanodine-receptor channels (RyR2), and SR Ca^{2+}-ATPase (Serca2a) was quantified by immunoblot, as previously described.[19] The phosphorylation-state of CaMKII (auto-phosphorylation-site Thr287), PLB (PKA-site Ser16; CaMKII-site Thr17), and RyR2 (PKA-site Ser2808; CaMKII-site Ser2814) was assessed with phospho-specific antibodies.

Computational Modeling

We developed a novel computational model of the human atrial cardiomyocyte based on work by Grandi et al.[20] and our recent model-extension.[21] Our model includes a spatial representation of Ca^{2+}-handling in the human atrial cardiomyocyte based on longitudinal division into ~2-μm-wide segments, and transverse division into ~1-μm-long domains. We recently showed that stochastic channel-gating is important for accurate simulation of cardiac dynamics, including Ca^{2+}-handling abnormalities.[22] Accordingly, we included stochastic gating of RyR2 based on experimental single-channel recordings.[15] The formulation of several ionic currents was updated to reproduce experimentally-observed Ca^{2+}-handling properties (see online supplement). The model was implemented in C++ and compiled using MinGW (model code available at http://www.uni-due.de/pharmakologie/). The effects of tetracaine and caffeine were simulated by reducing RyR2 open-probability by 90% and setting the open probability to 100%, respectively.

Statistical Analysis

Data were analyzed with multi-level mixed-effects models to take into account correlations between multiple levels of within-patient measurements. The generalized estimating equation (GEE) approach was performed using the binomial distribution to study the dichotomous spontaneous SR Ca^{2+}-release event and DAD outcomes. When analyses were performed for multiple cells/patient, the unit used for analysis was the independent variable patient-ID. For experiments in which there was only one measure per patient, oneway ANOVA was used to compare the groups. When applicable, heterogeneity of variance was accounted for in the models. All analyses were performed with SAS 9.3 (SAS Institute, Cary, North Carolina). Data are reported as mean±SEM. When multiple recordings are available from some subjects, sample-sizes are given as n/N, where n=cells and N=patients.

Results

Basic Electrophysiological Properties

AP-recordings showed no significant group-differences in AP-duration (APD) at 20%, 50%, and 90% repolarization (Figure 1A,B), indicating the absence of AF-associated electrical remodeling, consistent with the prolonged interval since the last AF-episode. Resting membrane potential and AP-amplitude were also similar (Figure 1C).

We then simultaneously recorded depolarization-induced $I_{Ca,L}$ and Ca^{2+}-transients under voltage-clamp conditions. In agreement with the unaltered APD, we found no significant difference in $I_{Ca,L}$ (Figure 2A,B). However, we observed an increased Ca^{2+}-transient amplitude (282.1±39.3 nmol/L vs. 183.9±15.2 nmol/L; P=0.070; Figure 2C) and accelerated time-constant of Ca^{2+} decay (τ = 215.3±20.6 ms vs. 315.8±26.8 ms; P=0.030; Figure 2D) in pAF (n/N=15/9) versus Ctl (n/N=35/25). These findings suggest a potential role for altered Ca^{2+}-handling in pAF-pathophysiology.

Incidence of Spontaneous SR Ca^{2+}-release Events

We assessed the occurrence of abnormal spontaneous SR Ca^{2+}-release events (SCaEs) and DADs/triggered activity under current-clamp conditions in the presence of physiological

bath Ca^{2+}-concentrations (2.0 mmol/L). SCaEs were defined as unstimulated rises in $[Ca^{2+}]_i$ following a 1-minute period of AP-triggered Ca^{2+}-transients. Potentially-arrhythmogenic DADs were defined as SCaE-induced membrane depolarizations exceeding 20 mV. The susceptibility to DADs (i.e., the percentage of cells showing DADs) was significantly increased in pAF (Figure 3A,B). The proportion of cells with SCaEs, as well as their intrinsic frequency and amplitude, was numerically greater, without statistical significance, in pAF (Figure 3C, left). SCaE-induced membrane depolarizations were significantly larger in pAF (Figure 3C).

SR Ca^{2+}-Uptake and Ca^{2+}-Content

The increased Ca^{2+}-transient amplitude in pAF despite unaltered 'trigger' $I_{Ca,L}$ suggests either enhanced SR Ca^{2+}-load or increased Ca^{2+}-sensitivity of RyR2. To assess the possibility of increased SR Ca^{2+}-load, we applied caffeine to open RyR2 and release all available Ca^{2+} from the SR. Quantification of the amplitude of caffeine-induced Ca^{2+}-transients provides a measure of SR Ca^{2+}-content, and was significantly increased in pAF (Figure 4A,B).[17] Consistently, charge carried by NCX1 was also numerically increased (P=0.109; Figure 4B). In contrast, the time-constant of caffeine-induced Ca^{2+}-transient decay (a measure of NCX function) was similar (Figure 4C). The slope of the line relating I_{NCX} to $[Ca^{2+}]_i$ (indicating the Ca^{2+}-dependent activation of NCX) (Figure 4D,E) showed no differences between groups, confirming unaltered NCX function in pAF. Furthermore, atrial NCX1 protein-expression was similar for Ctl versus pAF-patients (Figure 4F).

Increased SR Ca^{2+}-uptake by Serca2a could explain the augmentation of SR Ca^{2+}-content. Serca2a protein-expression was downregulated in pAF (Figure 5A), which would tend to reduce SR Ca^{2+}-uptake. However, PKA-phosphorylation (at Ser16) of the Serca2a-inhibitor PLB was significantly increased (Figure 5A), which should relieve PLB-induced Serca2a inhibition and increase SR Ca^{2+}-uptake. We determined expression of PKA catalytic and RII-regulatory subunits, total and Thr287- autophosphorylated CaMKII, calmodulin and protein phosphatase-type-1 and type-2A expression to identify potential upstream factors contributing to increased Ser16-PLB phosphorylation, but found no significant differences between Ctl and pAF-patients (Online Figures II-III). To assess net functional consequences of the altered protein-expression and phosphorylation, we calculated the Serca2a uptake-rate based on the rates of $I_{Ca,L}$-triggered Ca^{2+}-transient decay (reflecting extrusion by both NCX1 and Serca2a) and the caffeine-triggered Ca^{2+}-transient decay (reflecting Ca^{2+}-extrusion via NCX1), as previously described.[15, 23] We noted a significant increase in Serca2a-mediated SR Ca^{2+}-uptake in pAF (Figure 5B,C), suggesting that the increased SR Ca^{2+}-load may be at least partly attributable to enhanced Serca2a-function.

RyR2-function

We next assessed SR Ca^{2+}-leak with the tetracaine-method of Shannon et al.[18] (Figure 6A), whereby SR Ca^{2+}-leak is quantified as the drop in $[Ca^{2+}]_i$ when RyR2 channels are blocked with tetracaine in cardiomyocytes clamped at –80 mV and perfused with Na^+-/Ca^{2+}-free bath solution to prevent trans-sarcolemmal ion fluxes. Application of caffeine was used to assess SR Ca^{2+}-load under the same conditions. SR Ca^{2+}-leak was increased in pAF (59.6±8.5 nmol/L, n=6/3) versus Ctl (31.6±6.1 nmol/L, n/N=9/3; P=0.023). The pAF-related

increase in SR Ca^{2+}-leak could be due to intrinsic RyR2 dysregulation or to increased SR Ca^{2+}-load (2051.6±290.8 nmol/L, n=6/3) versus Ctl (1158.4±168.3 nmol/L, n=9/3; P=0.019; Figure 6C). Therefore, we assessed RyR2-expression and phosphorylation-levels by Western-blotting, and RyR2 single-channel properties in lipid-bilayers. RyR2 protein-expression was significantly increased in both tissue-lysates and isolated SR-fractions (Figure 6D), with unaltered Ser2814-RyR2 and slightly reduced Ser2808-RyR2 phosphorylation (in SR fractions only). In addition, we found a significantly-increased single-channel open-probability of RyR2 from pAF-patients (0.007±0.003, n=8/4 vs. 0.032±0.006, n/N=8/4; P=0.021; Figure 6E). These data suggest that both increased numbers of channels and enhanced single-channel open-probability could contribute to the increased SR Ca^{2+}-leak in pAF.

Computational Modeling of Atrial Ca^{2+}-Handling in Ctl and pAF

To further probe the role of altered RyR2 and Serca2a functions and associated SR Ca^{2+}-load increases in pAF-related Ca^{2+}-handling abnormalities, we developed a novel computational model of Ca^{2+}-handling in human atrial cardiomyocytes (Figure 7A). The model can be used to simulate patch-clamp and pharmacological protocols employed experimentally to assess Ca^{2+}-handling properties, and allows visualization of the spatial distribution of $[Ca^{2+}]_i$ in movies or line-scan representations (Figure 7B). Parameters of the Ctl model were optimized to reproduce a wide range of human atrial-cardiomyocyte Ca^{2+}-handling properties, including: $I_{Ca,L}$-amplitude; amplitude and decay time-constant of $I_{Ca,L}$-triggered Ca^{2+}-transients; SR Ca^{2+}-leak; amplitude of caffeine-induced Ca^{2+}-transient; and time-constant of caffeine-induced Ca^{2+}-transient decay (Figure 7C; Online Figures IV-VI). Incorporation of pAF-dependent alterations in Serca2a and RyR2 functions (Online Table IV) reproduced experimentally-observed Ca^{2+}-handling properties (Online Figure VII).

The control model with stochastic RyR2-gating showed isolated SCaEs when clamped at −80 mV following repeated depolarizing voltage-clamp steps to achieve steady-state SR Ca^{2+}-loading (Figure 8A). Incorporating either the pAF-related increase in SR Ca^{2+}-uptake or RyR2 dysregulation (increased expression and open-probability) increased the incidence of SCaEs. A combination of both alterations in the pAF model produced synergistic effects on SCaEs, with pronounced increases in their incidence and amplitudes, resulting in larger transient-inward currents (Figure 8B; Online Figure VIII). Simulated application of tetracaine and caffeine provided quantification of SR Ca^{2+}-leak and SR Ca^{2+}-load, respectively, in line with experimental protocols. Incorporating the pAF-related alterations in SR Ca^{2+}-uptake produced a significant increase in SR Ca^{2+}-load and SR Ca^{2+}-leak, whereas RyR2 dysregulation produced increased SR Ca^{2+}-leak despite reduced SR Ca^{2+}-load (Figure 8C). A combination of both alterations in the pAF model resulted in increased SR Ca^{2+}-load and a much larger SR Ca^{2+}-leak, in agreement with our experimental findings. Our computational modeling indicates that both increased SR Ca^{2+}-uptake and RyR2-dysregulation likely contribute to the greater incidence of SCaEs/DADs that we observed in pAF-cardiomyocytes. As an initial look at potential therapeutic implications, we simulated RyR2-inhibition by flecainide, which produced a dose-dependent reduction in SCaE-incidence (Online Figures IX-X), suggesting that inhibition of RyR2 could contribute to flecainide's antiarrhythmic properties in pAF.

Discussion

In the present study, we observed increased spontaneous cellular activity in atrial cardiomyocytes from pAF-patients, and analyzed the underlying cellular and molecular mechanisms. Our data showed an absence of AF-associated electrical remodeling like APD-abbreviation or $I_{Ca,L}$-reduction in pAF-cardiomyocytes. In contrast, experimental observations revealed an increased incidence of DADs due to RyR2 dysregulation and increased SR Ca^{2+}-uptake, resulting in enhanced SR Ca^{2+}-load. Computational modeling confirmed that these Ca^{2+}-handling abnormalities are sufficient to increase the incidence and amplitude of potentially arrhythmogenic DADs leading to cellular triggered activity. Together, these data point to Ca^{2+}-dependent triggered activity underlying atrial arrhythmogenesis in pAF-patients and identify potential culprit mechanisms.

Comparison with Previous Studies of AF-Associated Remodeling

The very rapid, irregular atrial activation in AF induces electrical remodeling, shortening atrial refractory periods and promoting reentry, contributing to the vicious cycle of "AF begets AF".[24] Downregulation of $I_{Ca,L}$ and upregulation of the inward-rectifier K^+-current I_{K1} are major components of the AF-induced electrical remodeling that abbreviates APD. Here, we found no differences in APD between pAF and Ctl-patients, indicating the absence of electrical-remodeling indicators in pAF-patients. These findings agree with previous work showing unchanged L-type Ca^{2+}-channel α_{1C}-subunit expression[25] and unchanged I_{K1} in right-atrial myocytes of pAF-patients.[13] Although downregulation of K^+-channel subunits (Kv4.3, Kv1.5, Kir3.1) has been described in atrial tissue from pAF-patients, which would be expected to prolong APD,[26] these changes may have been due to the underlying heart disease rather than pAF per se.[5, 26] In addition, the longer interval since the last pAF-episode in the current study (median of 10-20 days) compared to the work of Brundel et al. (median of 1.5 days)[26] suggests that any AF-induced electrical remodeling changes were reversed by the time of tissue procurement in our study and perhaps not in the Brundel investigation.

We and others have shown that long-standing persistent (chronic) AF (cAF) is associated with pronounced Ca^{2+}-handling abnormalities.[15, 27, 28] Here, we studied for the first time Ca^{2+}-handling properties in pAF. Although the incidence of SCaEs is increased in both pAF and cAF patients, the underlying molecular mechanisms appear distinct. In particular, activity of CaMKII is increased in patients with cAF, resulting in hyperphosphorylation of RyR2.[15, 28-30] RyR2 hyperphosphorylation increases channel open-probability and promotes SR Ca^{2+}-leak and SCaEs. In pAF, we found no increase in RyR2-phosphorylation. Nonetheless, there was an increase in single-channel RyR2 open-probability, perhaps due to other posttranslational modifications of RyR2 (e.g., oxidation, S-nitrosylation). In addition, the levels of certain RyR2-stabilizing subunits such as calsequestrin-2 and junctophilin-2 are not upregulated in pAF,[14] whereas here we noted upregulation of RyR2-expression. The increase in RyR2 without change in the associated regulator-proteins calsequestrin-2 and junctophilin-2 would cause relative depletion of such proteins in the RyR2-complex, potentially enhancing channel-activity.[14] SR Ca^{2+}-uptake was increased in pAF (opposite to the decrease in cAF), and the consequent enhancement in SR Ca^{2+}-load promotes greater SR

Ca^{2+}-leak and a higher frequency of SCaEs and DADs. In cAF, NCX1-expression is increased, producing larger depolarizing inward current for a given amount of free intracellular Ca^{2+}.[15] In contrast, NCX1 expression and its Ca^{2+}-dependent activation were unaltered in pAF. These differences in the mechanisms underlying Ca^{2+}-handling abnormalities in pAF versus cAF suggest that specific molecular signatures characterize the different forms of clinical AF, potentially allowing the development of more specific, patient-tailored therapeutic strategies. Of note, the same phenomenological endpoint (increased SR Ca^{2+}-leak, DADs and triggered activity) can result from quite distinct pathophysiological mechanism-complexes in different forms of AF, emphasizing the importance of understanding the underlying specifics of Ca^{2+}-handling dysregulation rather than simply studying final common heterostatic manifestations.

Computational modeling has proven useful to elucidate the fundamental mechanisms of atrial arrhythmias.[31] However, most currently-available atrial-cardiomyocyte models do not consider differences in subcellular structure between atrial and ventricular myocytes.[20, 31] In particular, the absence of a pronounced T-tubular network in atrial-cardiomyocytes has a major impact on Ca^{2+}-wave propagation. Recent models have started to incorporate atrial-specific subcellular structures to analyze Ca^{2+}-wave propagation.[32, 33] However, none of these models addressed the importance of SR Ca^{2+}-leak or the dynamics of abnormal SR Ca^{2+}-release in human atrial cardiomyocytes. Our newly-developed model adds multiple novel components to the recently-described model of the human atrial cardiomyocyte developed by Grandi et al:[20] (1) a subcellular structure able to simulate atrial-specific Ca^{2+}-wave propagation; (2) stochastic gating of RyR2-channels based on single-channel recordings; and (3) an improved representation of the L-type Ca^{2+}-channel, reproducing activation and inactivation properties measured in human atrial cardiomyocytes. Using this novel computational model, we were able to demonstrate that the experimentally-observed alterations in SR Ca^{2+}-uptake and RyR2 function account for the alterations in Ca^{2+}-handling and greater incidence of SCaEs that we observed in pAF-cardiomyocytes.

Novel Findings and Potential Clinical Implications

Despite substantial progress in our understanding of AF-pathophysiology, the arrhythmogenic mechanisms leading to the spontaneously self-terminating AF-episodes typical of pAF-patients remained elusive. To the best of our knowledge, we provide the first comprehensive study addressing potential Ca^{2+}-related cellular and molecular atrial proarrhythmic mechanisms in pAF-patients. Although reentry and focal Ca^{2+}-driven ectopic activity have been postulated to be potential contributors to pAF-pathophysiology, direct experimental evidence at the cellular level has been lacking. We did not observe any indices of AF-induced electrical remodeling, such as APD-shortening and $I_{Ca,L}$-reduction, in pAF-patients. In contrast, our data suggest that SCaEs and corresponding DADs associated with enhanced SR Ca^{2+}-uptake and intrinsic RyR2 dysregulation may represent the cellular correlates of the clinically-observed focal ectopic (triggered) activity that triggers and may even maintain AF-recurrences in pAF-patients.

Our previous and current data suggest that increased diastolic SR Ca^{2+}-leak is a common motif in both pAF and cAF, although the underlying molecular basis and the

pathophysiological role are likely distinct for each form of the arrhythmia. Patients with pAF do not have atrial tachycardia-induced remodeling and can usually be successfully treated by targeting of PV-triggers.[12] The mechanism underlying PV trigger-activity has been elusive. Our results indicate that in pAF-patients, increased SR Ca^{2+}-leak and incidence of diastolic SR Ca^{2+}-release events promote cellular DADs and triggered activity, which, if they occur synchronously in a critical number of cardiomyocytes, might cause triggered activity that underlies AF-episodes. Our data also suggest that increased SR Ca^{2+}-load due to enhanced SR Ca^{2+}-uptake conspires with RyR2 dysregulation to increase SR Ca^{2+}-leak and cause SCaEs in pAF-patients. Since our model indicates that either increased SR Ca^{2+}-uptake or RyR2 dysregulation can also increase SCaEs incidence individually, pharmacological approaches to pAF may need to target both components, in contrast to cAF, in which targeting RyR2-hyperphosphorylation alone may be sufficient to suppress SCaEs. New pharmacological approaches to Ca^{2+}-handling abnormalities in pAF might allow for more effective targeting in the early paroxysmal stages of the disorder, before the otherwise inexorable progression to more resistant forms occurs.[4]

Here we used a newly-developed computational model, which is the first human atrial cardiomyocyte model able to simulate potentially-arrhythmogenic SCaEs. Importantly, the model was extensively validated based on simultaneous ion-current and $[Ca^{2+}]_i$-recordings at physiological temperature in human atrial myocytes.[15, 16] Taking advantage of these improvements, we also provide the first computational model of atrial cardiomyocytes in pAF, which reproduces key pAF-specific alterations in atrial Ca^{2+}-handling properties.

Although SR Ca^{2+}-leak is typically seen in cAF-patient cardiomyocytes,[15, 27, 28] it is unclear what functional role DADs/triggered activity plays in their arrhythmia, given its sustained nature and the underlying complex, reentry-maintaining substrate. In such individuals, increased SR Ca^{2+}-leak may contribute indirectly by producing progressive Ca^{2+}-dependent electrical and structural remodeling. There is accumulating evidence that RyR2 dysregulation can promote reentry through remodeling of Na^+-channels and intercellular connexins.[34, 35] Abnormal Ca^{2+}-handling in cAF may also modulate other ion-channels, potentially shortening APD by activating SK-channels[36] or favoring development of constitutive $I_{K,ACh}$ activity,[37] or contributing to repolarization alternans, which has been associated with AF vulnerability in persistent AF.[38] Finally, RyR2 dysregulation has also been associated with worse structural remodeling following cardiac injury,[39] suggesting that cAF-dependent Ca^{2+}-handling abnormalities can promote reentry via atrial structural remodeling. Although the potential arrhythmogenic role of SR Ca^{2+}-leak is much more obvious in pAF than cAF, even in pAF cytosolic SR Ca^{2+}-leaks could contribute to remodeling and the development of a reentry substrate leading to progression to persistent and long-lasting persistent forms.

Potential Limitations

Because of limited availability of human tissue, only right-atrial appendages were employed in this study. Other atrial regions, notably the peri-PV left atrium, may play a more prominent role in ectopic activity and reentry (with left-to-right dominance of rotor frequencies).[2] Thus, we cannot exclude that other mechanisms may contribute to pAF-

initiation in these other regions. For example, we previously showed that the inward-rectifier K^+-current is increased in left, but not right, atrial myocytes from pAF-patients.[13] Nevertheless, right-atrial arrhythmogenic sites clearly occur and can represent 1/3 of all AF-generators in AF-patients.[40] In addition, there were some small intergroup differences with respect to age and the incidence of diabetes, which should be considered in interpreting our results.

Here, we identified potential arrhythmogenic mechanisms in isolated atrial cardiomyocytes from pAF-patients. There are numerous additional factors (genetic, autonomic, inflammatory, structural) that may modulate arrhythmic risk in vivo and we are in no way claiming that the properties studied here account fully for any clinical arrhythmic phenotype. In addition, we did not assess structural alterations or remodeling of connexins that may promote reentry and contribute to pAF. Interestingly, left-atrial diameter of pAF-patients was not substantially enlarged (mean 43 mm) and was not significantly different from controls (Online Tables I-III), suggesting the absence of any important structural remodeling in our pAF-population. Furthermore, recent work demonstrated no increases in global atrial fibrosis in pAF.[41] In addition, RyR2 mutations underlying catecholaminergic polymorphic ventricular tachycardia have also been associated with Ca^{2+}-handling abnormalities and pAF in the absence of structural heart disease,[42, 43] suggesting that SR Ca^{2+}-leak-related DAD/triggered activity mechanisms of the type identified in our study can be sufficient to underlie pAF.

The individuals from whom we obtained tissue-samples of necessity included only patients that underwent open-heart surgery for coronary bypass grafting and/or valve replacement. Such individuals have numerous co-morbidities. The phenotype of atrial cardiomyocytes from our Ctl-patients may be different from non-diseased controls and it is unclear whether the pAF mechanisms identified here also apply to pAF-patients without any heart disease. Of necessity, information about AF-type and timing were obtained from the clinical chart. While it would be very useful to perform the types of analyses described here in a population with routine prospective long-term rhythm-recording prior to surgery in order to relate the precise duration and frequency of AF-episodes to the ionic and molecular phenotype, such a study is practically extremely difficult and was impossible for us. The limited nature of our AF-characterization must be considered in interpreting our results. It has been suggested that at least two types of pAF are likely to exist.[2] The first is characterized by frequent short-lived episodes which may result from a repetitive ectopic trigger. The second type generally persists longer (>24 h) and recurs less frequently. The latter type is likely associated with a reentrant mechanism. Whether, as one might expect, the arrhythmogenic mechanisms identified in the present study are associated with particular clinical presentations needs prospective evaluation in future studies. If the phenotype observed here is a common unifying theme in pAF, it will be important to determine the specific underlying molecular abnormalities. In particular, the analysis of the precise molecular mechanisms contributing to increased RyR2 protein-expression and greater channel open probability, along with enhanced Serca2a activity, are beyond the scope of the current project and should be addressed in future detailed studies.

Conclusions

In this study, we evaluated the cellular and molecular determinants of intracellular Ca^{2+}-handling in pAF-patients, and observed an increased incidence of SCaEs due to increased SR Ca^{2+}-load and RyR2 dysregulation, causing DADs and triggered activity. The underlying molecular basis appeared to be enhanced SR Ca^{2+}-uptake caused by PLB-hyperphosphorylation, and increased expression and open-probability of RyR2. The novel experimental and computational insights we obtained into fundamental arrhythmogenic mechanisms in pAF may facilitate the development of safer and more effective mechanism-based therapeutic strategies.

Supplementary Material

Refer to Web version on PubMed Central for supplementary material.

Acknowledgements

References

1. Go AS, Mozaffarian D, Roger VL, Benjamin EJ, Berry JD, Borden WB, Bravata DM, Dai S, Ford ES, Fox CS, Franco S, Fullerton HJ, Gillespie C, Hailpern SM, Heit JA, Howard VJ, Huffman MD, Kissela BM, Kittner SJ, Lackland DT, Lichtman JH, Lisabeth LD, Magid D, Marcus GM, Marelli A, Matchar DB, McGuire DK, Mohler ER, Moy CS, Mussolino ME, Nichol G, Paynter NP, Schreiner PJ, Sorlie PD, Stein J, Turan TN, Virani SS, Wong ND, Woo D, Turner MB. Heart disease and stroke statistics-2013 update: a report from the American Heart Association. Circulation. 2013; 127:e6–e245. [PubMed: 23239837]

2. Nattel S. Paroxysmal Atrial Fibrillation and Pulmonary Veins: Relationships Between Clinical Forms and Automatic vs Re-entrant Mechanisms. Can J Cardiol. 2013; 29:1147–1149. [PubMed: 23993351]

3. Camm AJ, Al-Khatib SM, Calkins H, Halperin JL, Kirchhof P, Lip GY, Nattel S, Ruskin J, Banerjee A, Blendea D, Guasch E, Needleman M, Saveliyeva I, Viles-Gonzalez J, Williams ES. A proposal for new clinical concepts in the management of atrial fibrillation. Am Heart J. 2012; 164:292–302. e291. [PubMed: 22980294]

4. Van Gelder IC, Hemels ME. The progressive nature of atrial fibrillation: a rationale for early restoration and maintenance of sinus rhythm. Europace. 2006; 8:943–949. [PubMed: 16973685]

5. Dobrev D, Carlsson L, Nattel S. Novel molecular targets for atrial fibrillation therapy. Nat Rev Drug Discov. 2012; 11:275–291. [PubMed: 22460122]

6. Heijman J, Voigt N, Dobrev D. New directions in antiarrhythmic drug therapy for atrial fibrillation. Future Cardiol. 2013; 9:71–88. [PubMed: 23259476]

7. Wakili R, Voigt N, Kaab S, Dobrev D, Nattel S. Recent advances in the molecular pathophysiology of atrial fibrillation. J Clin Invest. 2011; 121:2955–2968. [PubMed: 21804195]

8. Nattel S, Burstein B, Dobrev D. Atrial remodeling and atrial fibrillation: mechanisms and implications. Circ Arrhythm Electrophysiol. 2008; 1:62–73. [PubMed: 19808395]

9. Nattel S, Shiroshita-Takeshita A, Brundel BJ, Rivard L. Mechanisms of atrial fibrillation: lessons from animal models. Prog Cardiovasc Dis. 2005; 48:9–28. [PubMed: 16194689]

10. Wijffels MC, Kirchhof CJ, Dorland R, Allessie MA. Atrial fibrillation begets atrial fibrillation. A study in awake chronically instrumented goats. Circulation. 1995; 92:1954–1968. [PubMed: 7671380]

11. Wakili R, Yeh YH, Yan Qi X, Greiser M, Chartier D, Nishida K, Maguy A, Villeneuve LR, Boknik P, Voigt N, Krysiak J, Kääb S, Ravens U, Linke WA, Stienen GJ, Shi Y, Tardif JC, Schotten U, Dobrev D, Nattel S. Multiple potential molecular contributors to atrial hypocontractility caused by atrial tachycardia remodeling in dogs. Circ Arrhythm Electrophysiol. 2010; 3:530–541. [PubMed: 20660541]

12. Haissaguerre M, Jais P, Shah DC, Takahashi A, Hocini M, Quiniou G, Garrigue S, Le Mouroux A, Le Metayer P, Clementy J. Spontaneous initiation of atrial fibrillation by ectopic beats originating in the pulmonary veins. N Engl J Med. 1998; 339:659–666. [PubMed: 9725923]

13. Voigt N, Trausch A, Knaut M, Matschke K, Varro A, Van Wagoner DR, Nattel S, Ravens U, Dobrev D. Left-to-right atrial inward rectifier potassium current gradients in patients with paroxysmal versus chronic atrial fibrillation. Circ Arrhythm Electrophysiol. 2010; 3:472–480. [PubMed: 20657029]

14. Beavers DL, Wang W, Ather S, Voigt N, Garbino A, Dixit SS, Landstrom AP, Li N, Wang Q, Olivotto I, Dobrev D, Ackerman MJ, Wehrens XH. Mutation E169K in junctophilin-2 causes atrial fibrillation due to impaired RyR2 stabilization. J Am Coll Cardiol. 2013 doi:10.1016/j.jacc. 2013.06.052.

15. Voigt N, Li N, Wang Q, Wang W, Trafford AW, Abu-Taha I, Sun Q, Wieland T, Ravens U, Nattel S, Wehrens XH, Dobrev D. Enhanced sarcoplasmic reticulum Ca^{2+} leak and increased Na^+-Ca^{2+} exchanger function underlie delayed afterdepolarizations in patients with chronic atrial fibrillation. Circulation. 2012; 125:2059–2070. [PubMed: 22456474]

16. Voigt N, Zhou XB, Dobrev D. Isolation of human atrial myocytes for simultaneous measurements of Ca^{2+} transients and membrane currents. J Vis Exp. 2013; 77:e50235. [PubMed: 23852392]

17. Trafford AW, Diaz ME, Eisner DA. A novel, rapid and reversible method to measure Ca buffering and time-course of total sarcoplasmic reticulum Ca content in cardiac ventricular myocytes. Pflug Arch. 1999; 437:501–503.

18. Shannon TR, Ginsburg KS, Bers DM. Quantitative assessment of the SR Ca^{2+} leak-load relationship. Circ Res. 2002; 91:594–600. [PubMed: 12364387]

19. El-Armouche A, Boknik P, Eschenhagen T, Carrier L, Knaut M, Ravens U, Dobrev D. Molecular determinants of altered Ca^{2+} handling in human chronic atrial fibrillation. Circulation. 2006; 114:670–680. [PubMed: 16894034]

20. Grandi E, Pandit SV, Voigt N, Workman AJ, Dobrev D, Jalife J, Bers DM. Human atrial action potential and Ca^{2+} model: sinus rhythm and chronic atrial fibrillation. Circ Res. 2011; 109:1055–1066. [PubMed: 21921263]

21. Voigt N, Heijman J, Trausch A, Mintert-Jancke E, Pott L, Ravens U, Dobrev D. Impaired Na^+-dependent regulation of acetylcholine-activated inward-rectifier K^+ current modulates action potential rate dependence in patients with chronic atrial fibrillation. J Mol Cell Cardiol. 2013; 61:142–152. [PubMed: 23531443]

22. Heijman J, Zaza A, Johnson DM, Rudy Y, Peeters RL, Volders PG, Westra RL. Determinants of beat-to-beat variability of repolarization duration in the canine ventricular myocyte: a computational analysis. PLoS Comput Biol. 2013; 9:e1003202. [PubMed: 23990775]

23. Walden AP, Dibb KM, Trafford AW. Differences in intracellular calcium homeostasis between atrial and ventricular myocytes. J Mol Cell Cardiol. 2009; 46:463–473. [PubMed: 19059414]

24. Dobrev D. Electrical remodeling in atrial fibrillation. Herz. 2006; 31:108–112. quiz 142-103. [PubMed: 16738832]

25. Brundel BJ, van Gelder IC, Henning RH, Tuinenburg AE, Deelman LE, Tieleman RG, Grandjean JG, van Gilst WH, Crijns HJ. Gene expression of proteins influencing the calcium homeostasis in patients with persistent and paroxysmal atrial fibrillation. Cardiovasc Res. 1999; 42:443–454. [PubMed: 10533580]

26. Brundel BJ, Van Gelder IC, Henning RH, Tuinenburg AE, Wietses M, Grandjean JG, Wilde AA, Van Gilst WH, Crijns HJ. Alterations in potassium channel gene expression in atria of patients with persistent and paroxysmal atrial fibrillation: differential regulation of protein and mRNA levels for K^+ channels. J Am Coll Cardiol. 2001; 37:926–932. [PubMed: 11693772]

27. Hove-Madsen L, Llach A, Bayes-Genis A, Roura S, Rodriguez Font E, Aris A, Cinca J. Atrial fibrillation is associated with increased spontaneous calcium release from the sarcoplasmic reticulum in human atrial myocytes. Circulation. 2004; 110:1358–1363. [PubMed: 15313939]

28. Neef S, Dybkova N, Sossalla S, Ort KR, Fluschnik N, Neumann K, Seipelt R, Schondube FA, Hasenfuss G, Maier LS. CaMKII-Dependent Diastolic SR Ca^{2+} Leak and Elevated Diastolic Ca^{2+} Levels in Right Atrial Myocardium of Patients With Atrial Fibrillation. Circ Res. 2010; 106:1134–1144. [PubMed: 20056922]

29. Purohit A, Rokita AG, Guan X, Chen B, Koval OM, Voigt N, Neef S, Sowa T, Gao Z, Luczak ED, Stefansdottir H, Behunin AC, Li N, El Accaoui RN, Yang B, Swaminathan PD, Weiss RM, Wehrens XH, Song LS, Dobrev D, Maier LS, Anderson ME. Oxidized CaMKII Triggers Atrial Fibrillation. Circulation. 2013; 128:1748–1757. [PubMed: 24030498]

30. Chelu MG, Sarma S, Sood S, Wang S, van Oort RJ, Skapura DG, Li N, Santonastasi M, Muller FU, Schmitz W, Schotten U, Anderson ME, Valderrabano M, Dobrev D, Wehrens XH. Calmodulin kinase II-mediated sarcoplasmic reticulum Ca^{2+} leak promotes atrial fibrillation in mice. J Clin Invest. 2009; 119:1940–1951. [PubMed: 19603549]

31. Courtemanche M, Ramirez RJ, Nattel S. Ionic mechanisms underlying human atrial action potential properties: insights from a mathematical model. Am J Physiol. 1998; 275:H301–321. [PubMed: 9688927]

32. Koivumaki JT, Korhonen T, Tavi P. Impact of sarcoplasmic reticulum calcium release on calcium dynamics and action potential morphology in human atrial myocytes: a computational study. PLoS Comput Biol. 2011; 7:e1001067. [PubMed: 21298076]

33. Thul R, Coombes S, Roderick HL, Bootman MD. Subcellular calcium dynamics in a whole-cell model of an atrial myocyte. Proc Natl Acad Sci USA. 2012; 109:2150–2155. [PubMed: 22308396]

34. Heijman J, Wehrens XH, Dobrev D. Atrial arrhythmogenesis in catecholaminergic polymorphic ventricular tachycardia-is there a mechanistic link between sarcoplasmic reticulum Ca^{2+} leak and re-entry? Acta Physiol (Oxf). 2013; 207:208–211. [PubMed: 23157571]

35. King JH, Wickramarachchi C, Kua K, Du Y, Jeevaratnam K, Matthews HR, Grace AA, Huang CL, Fraser JA. Loss of Nav1.5 expression and function in murine atria containing the RyR2-P2328S gain-of-function mutation. Cardiovasc Res. 2013; 99:751–759. [PubMed: 23723061]

36. Diness JG, Sorensen US, Nissen JD, Al-Shahib B, Jespersen T, Grunnet M, Hansen RS. Inhibition of small-conductance Ca^{2+}-activated K^+ channels terminates and protects against atrial fibrillation. Circ Arrhythm Electrophysiol. 2010; 3:380–390. [PubMed: 20562443]

37. Makary S, Voigt N, Maguy A, Wakili R, Nishida K, Harada M, Dobrev D, Nattel S. Differential protein kinase C isoform regulation and increased constitutive activity of acetylcholine-regulated potassium channels in atrial remodeling. Circ Res. 2011; 109:1031–1043. [PubMed: 21903936]

38. Narayan SM, Franz MR, Clopton P, Pruvot EJ, Krummen DE. Repolarization alternans reveals vulnerability to human atrial fibrillation. Circulation. 2011; 123:2922–2930. [PubMed: 21646498]

39. Respress JL, van Oort RJ, Li N, Rolim N, Dixit SS, deAlmeida A, Voigt N, Lawrence WS, Skapura DG, Skardal K, Wisloff U, Wieland T, Ai X, Pogwizd SM, Dobrev D, Wehrens XH. Role of RyR2 phosphorylation at S2814 during heart failure progression. Circ Res. 2012; 110:1474–1483. [PubMed: 22511749]

40. Baykaner T, Clopton P, Lalani GG, Schricker AA, Krummen DE, Narayan SM. Targeted Ablation at Stable Atrial Fibrillation Sources Improves Success Over Conventional Ablation in High-Risk Patients: A Substudy of the CONFIRM Trial. Can J Cardiol. 2013; 29:1218–1226. [PubMed: 23993247]

41. van Brakel TJ, van der Krieken T, Westra SW, van der Laak JA, Smeets JL, van Swieten HA. Fibrosis and electrophysiological characteristics of the atrial appendage in patients with atrial fibrillation and structural heart disease. J Interv Card Electrophysiol. 2013; 38:85–93. [PubMed: 24026967]

42. Kazemian P, Gollob MH, Pantano A, Oudit GY. A novel mutation in the RYR2 gene leading to catecholaminergic polymorphic ventricular tachycardia and paroxysmal atrial fibrillation: dose-dependent arrhythmia-event suppression by beta-blocker therapy. Can J Cardiol. 2011; 27:870, e877–810. [PubMed: 21652165]

43. Zhabyeyev P, Hiess F, Wang R, Liu Y, Wayne Chen SR, Oudit GY. S4153R Is a Gain-of-Function Mutation in the Cardiac Ca^{2+} Release Channel Ryanodine Receptor Associated With Catecholaminergic Polymorphic Ventricular Tachycardia and Paroxysmal Atrial Fibrillation. Can J Cardiol. 2013; 29:993–996. [PubMed: 23498838]
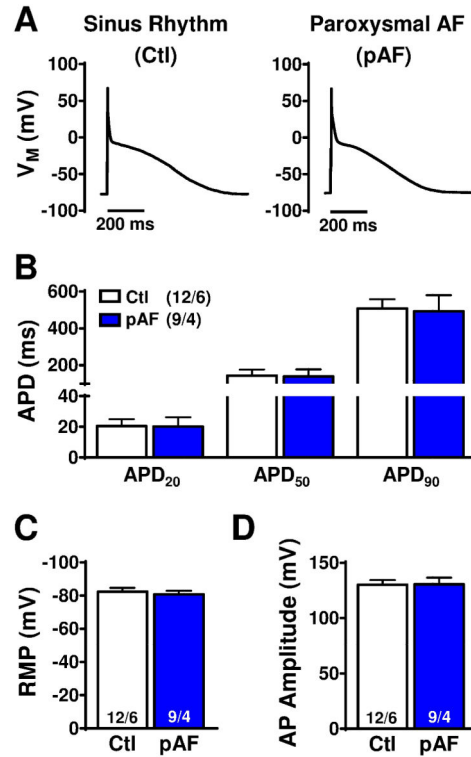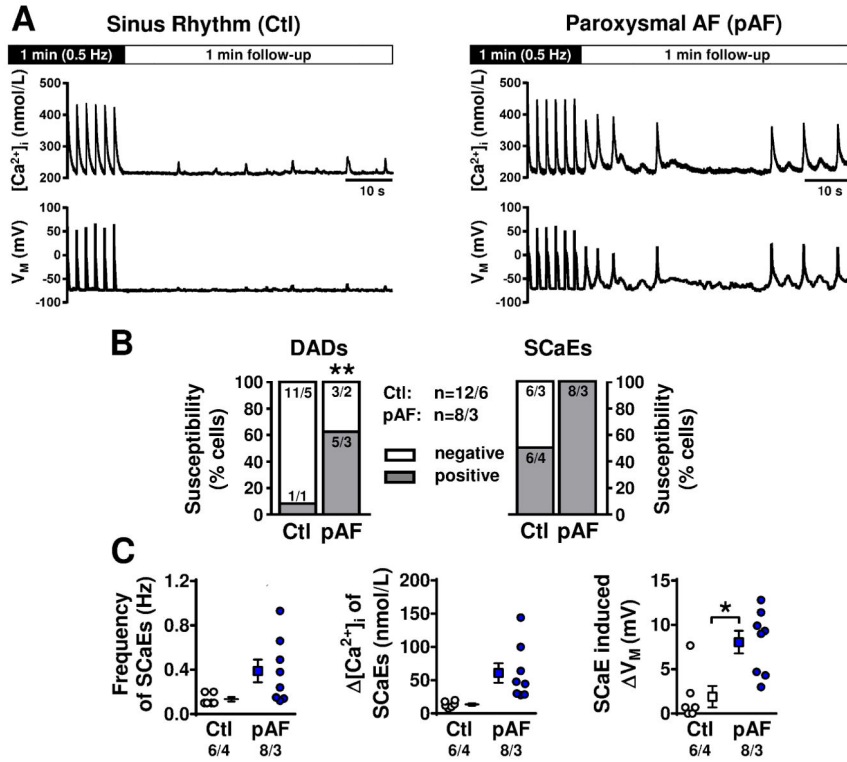
Figure 1.
Atrial-cardiomyocyte action-potential (AP) characteristics in sinus-rhythm (Ctl) or paroxysmal atrial fibrillation (pAF) patients. **A.** Atrial APs recorded at 0.5 Hz. **B.** AP-duration at 20%, 50%, and 90% repolarization (APD_{20}, APD_{50}, and APD_{90}). **C.** Resting membrane potential (RMP). **D.** AP-amplitude. n/N=numbers of myocytes/patients. Comparisons using multi-level mixed-effects models.
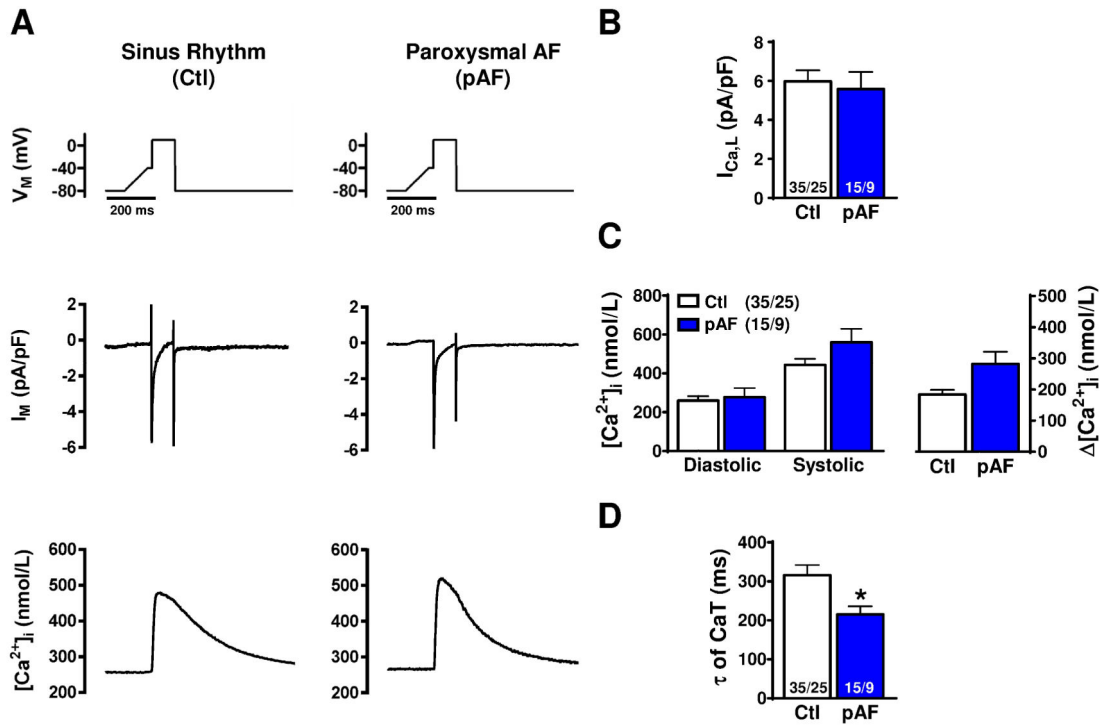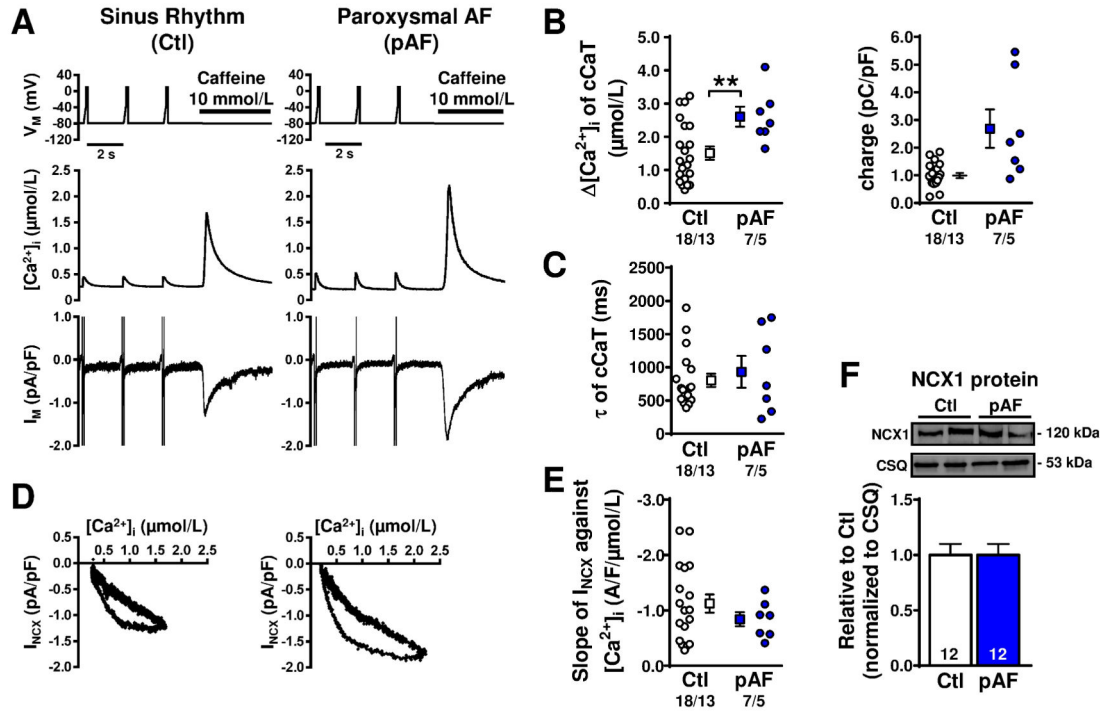
Figure 2.
L-type Ca^{2+}-current ($I_{Ca,L}$) and $I_{Ca,L}$-triggered Ca^{2+}-transient properties. **A.** Voltage-clamp protocol (V_m, applied at 0.5 Hz) and simultaneous recordings of $I_{Ca,L}$ (I_M) and $I_{Ca,L}$-triggered Ca^{2+}-transients (top to bottom) in a Ctl (left) or pAF (right) myocyte. **B.** Peak $I_{Ca,L}$-amplitude. **C.** Diastolic and systolic ($I_{Ca,L}$-triggered) Ca^{2+}-levels, and corresponding Ca^{2+}-transient ($[Ca^{2+}]_i$). **D.** Time-constant of Ca^{2+}-transient decay. *$P<0.05$ vs. Ctl. n/ N=numbers of myocytes/patients. Comparisons using multi-level mixed-effects models.
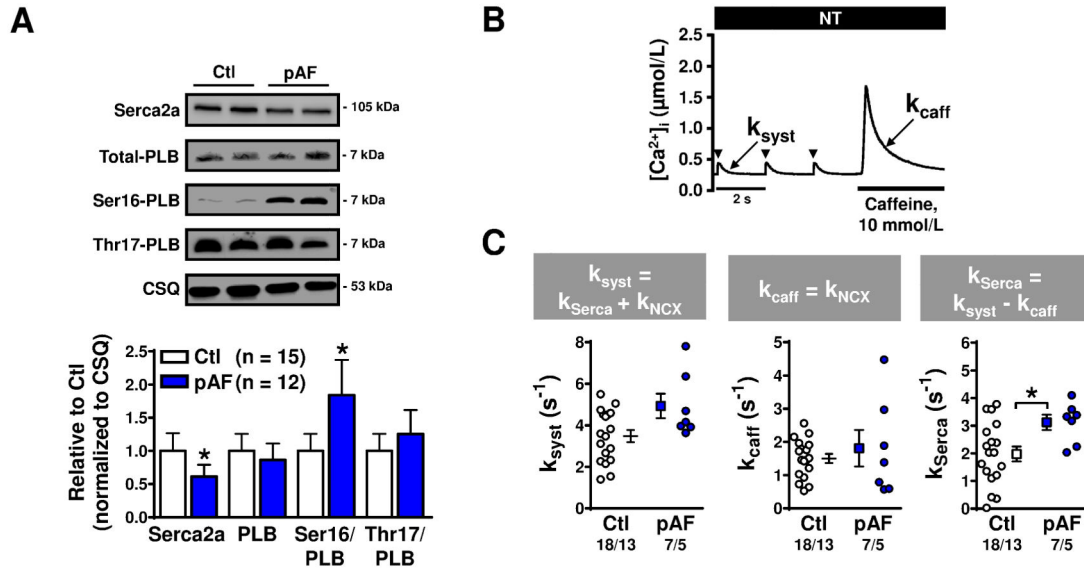
Figure 3.
Spontaneous SR Ca^{2+}-release events (SCaEs). **A.** Intracellular [Ca^{2+}] (top) and membrane potential (bottom) in Ctl (left) and pAF (right) cardiomyocytes. SCaEs and delayed afterdepolarizations (DADs) were assessed during a one-minute follow-up period after cessation of 0.5 Hz-stimulation in 2.0-mmol/L extracellular-[Ca^{2+}]. **B.** Prevalence of DADs exceeding 20 mV (left) and SCaEs (right). **C.** Intrinsic frequency of SCaEs (left), SCaE-amplitudes (middle) and corresponding membrane-potential changes (right). *P<0.05, **P<0.01 vs. Ctl. n/N=numbers of myocytes/patients. Comparisons using multi-level mixed-effects models.
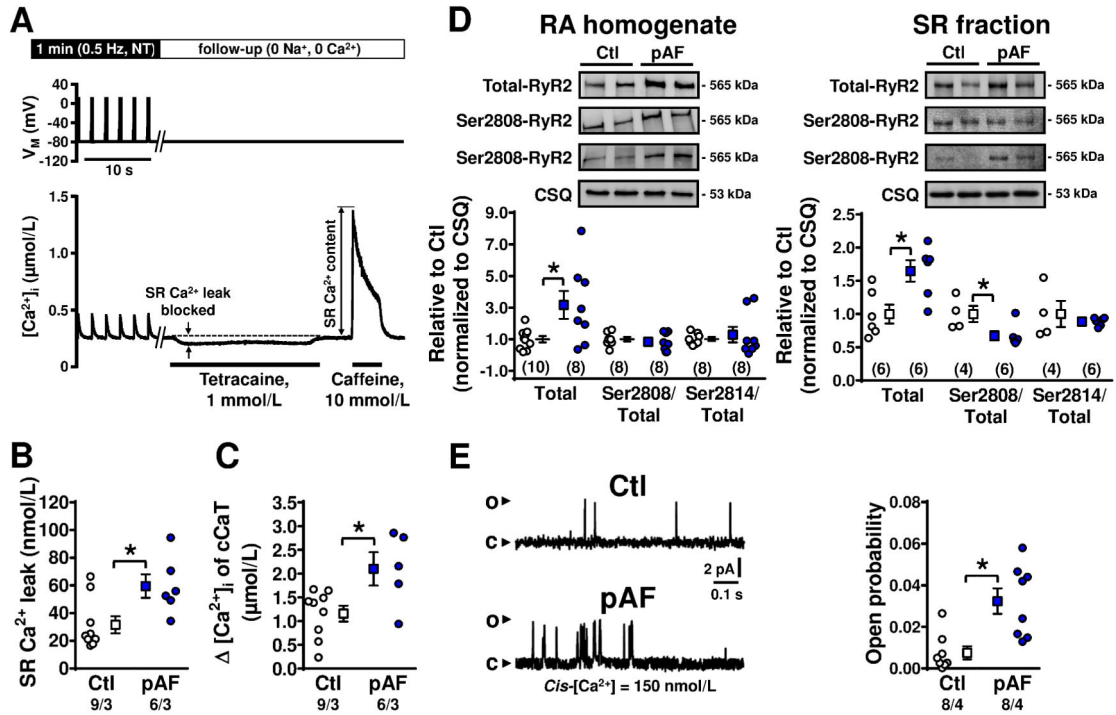
Figure 4.
SR Ca^{2+}-content and Na^+-Ca^{2+}-exchange (NCX) current (I_{NCX}) in atrial myocytes from Ctl and pAF-cardiomyocytes. **A.** Voltage-clamp protocol (top), and resulting $I_{Ca,L}$- and caffeine-triggered Ca^{2+}-transients (middle), or membrane-currents (I_m, bottom). **B.** SR Ca^{2+}-load, quantified with caffeine-triggered Ca^{2+}-transient amplitude (left), or integrated membrane-current (right). **C.** Time-constants of caffeine-triggered Ca^{2+}-transient decay (reflecting Ca^{2+}-extrusion via NCX). **D.** I_{NCX} as a function of $[Ca^{2+}]$. **E.** Ca^{2+}-dependence of NCX, based on slope of linear fit to the $I_{NCX}/[Ca^{2+}]_i$ relationship during the decay of the caffeine-triggered Ca^{2+}-transient. **F.** Representative Western blots (top) and mean NCX1 protein-expression (bottom) in atrial tissue-samples. Calsequestrin (CSQ) was loading-control. **$P<0.01$ vs. Ctl. n/N=numbers of myocytes/patients (B,C,E). N=number of tissue-samples (F). Comparisons using multi-level mixed-effects models (B,C,E) or one-way ANOVA (F).
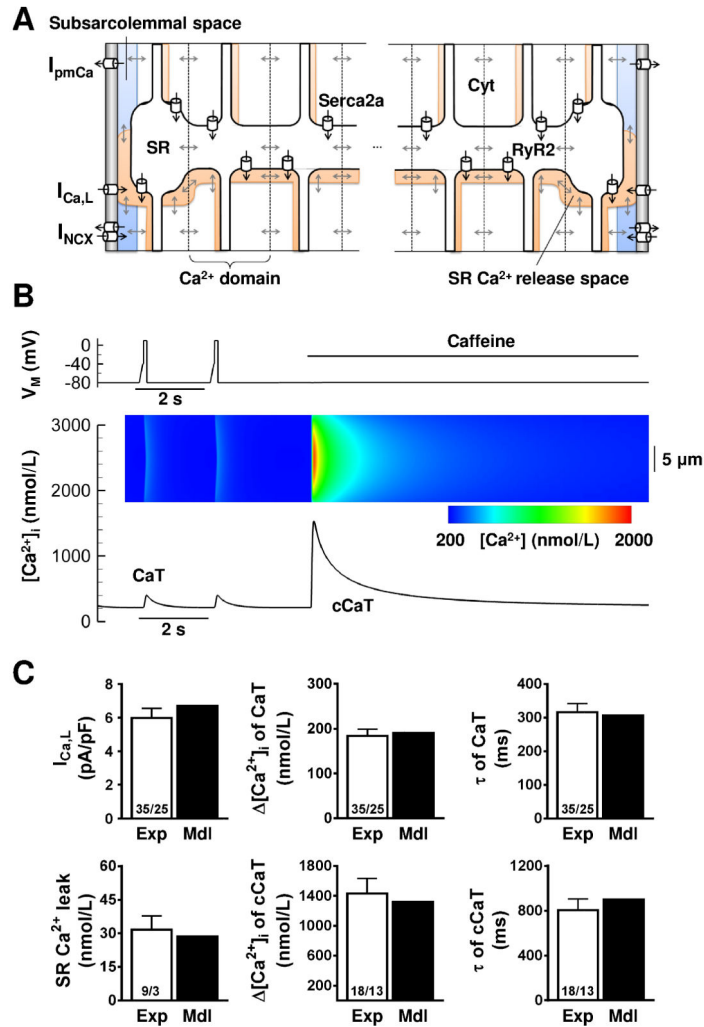
Figure 5.
SR Ca^{2+}-ATPase (Serca2a) and phospholamban (PLB) expression, phosphorylation and function in Ctl and pAF-patients. **A.** Representative Western blots (top) for total Serca2a and total PLB protein-expression, as well as Ser16-PLB phosphorylation, Thr17-PLB phosphorylation, and calsequestrin (CSQ) expression. Bottom panel shows quantification of total Serca2a and PLB expression, and relative Ser16/Thr17 PLB phosphorylation-levels. Group data are normalized to CSQ. **B.** Representative example of a caffeine experiment, highlighting the decay rate of the systolic ($I_{Ca,L}$-triggered) Ca^{2+}-transient (k_{syst}) and the decay rate of the caffeine-induced Ca^{2+}-transient (k_{caff}). **C.** Respective rate-constants k_{syst} (left), k_{caff} (middle) and k_{Serca} (right, obtained as the difference between k_{syst} and k_{caff}) in Ctl and pAF-patients. Numbers indicate tissue samples per group (panel A) or myocytes/patients (panel C). *$P<0.05$ vs. Ctl. Comparisons using one-way ANOVA (A) or multi-level mixed-effects models (C).
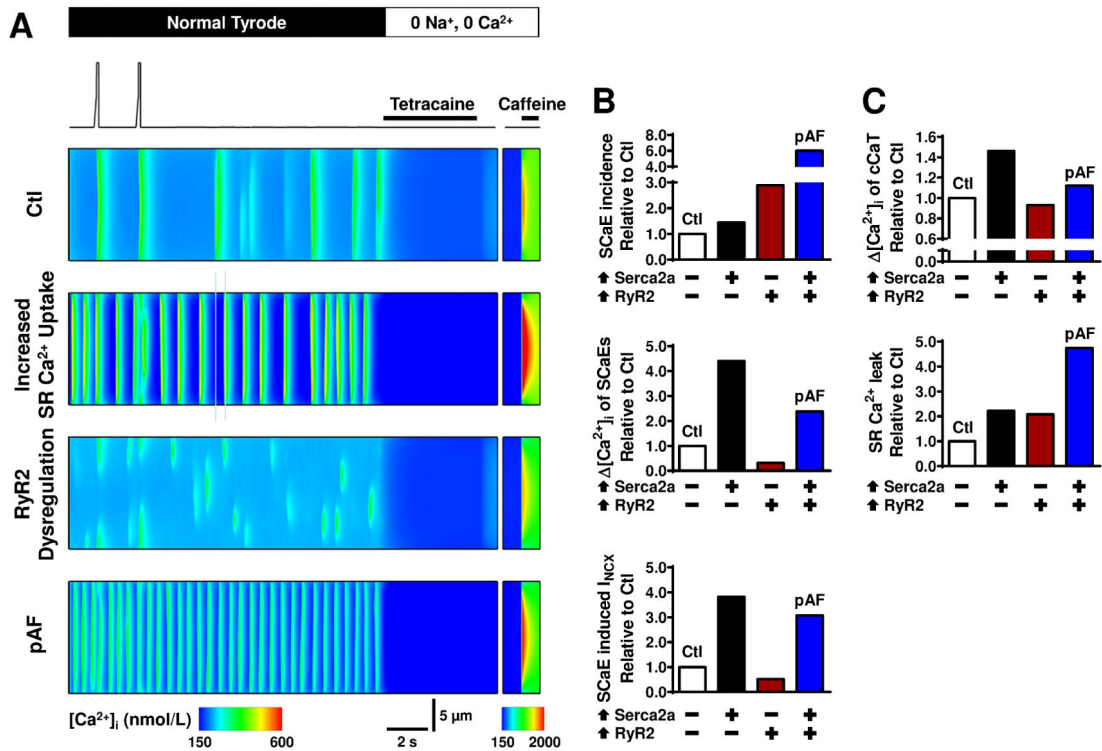
Figure 6.
SR Ca^{2+}-leak and ryanodine-receptor channel (RyR2) function in Ctl and pAF-patients. **A.** Voltage-clamp protocol (top) and $[Ca^{2+}]_i$ (bottom) in a representative Ctl experiment, illustrating the method for SR Ca^{2+}-leak and SR Ca^{2+}-content quantification in human atrial myocytes using the tetracaine protocol developed by Shannon et al.[18] **B.** Total SR Ca^{2+}-leak in Ctl and pAF-patients. **C.** SR Ca^{2+}-load quantified using caffeine-triggered Ca^{2+}-transient amplitude. **D.** Representative Western blots showing total RyR2, Ser2808- or Ser2814-phosphorylated RyR2 in tissue-homogenates (left) or SR-fractions (right). Bottom panels show total RyR2 expression and Ser2808 and Ser2814 phosphorylation levels (relative to total RyR2 expression) in corresponding Ctl and pAF-samples. **E.** Representative RyR2 single-channel recordings in lipid-bilayers showing channel openings (upward deflections) at 150 nmol/L cytosolic (*cis*) $[Ca^{2+}]$ in RyR2 isolated from Ctl or pAF-samples (left). RyR2 open-probability (P_o) in Ctl or pAF-samples (right). Data are shown relative to Ctl. Numbers indicate myocytes/patients (in panels B,C), tissue samples (panel D), or channels/patients (panel E). * $P<0.05$ versus Ctl. Comparisons using multi-level mixed-effects models (B,C,E) or one-way ANOVA (D).

Figure 7.
Computational modeling of human atrial Ca^{2+}-handling. **A.** Schematic of a single longitudinal segment, highlighting the 18 transverse Ca^{2+}-domains, subcellular Ca^{2+}-diffusion, subcellular compartments (Cyt: cytosol, SR: sarcoplasmic-reticulum, subsarc.: subsarcolemmal space), and Ca^{2+}-transport mechanisms (Serca2a: SR Ca^{2+}-ATPase; RyR2: ryanodine-receptor channel type-2; $I_{Ca,L}$: L-type Ca^{2+}-current; I_{NCX}: Na$^+$-Ca^{2+}-exchange current; I_{pmCa}: plasmalemmal Ca^{2+}-ATPase). Ca^{2+}-buffers and other ion-currents are also incorporated into the model but omitted here for clarity. **B.** Experimental voltage-clamp protocol (top), along with simulated whole-cell $I_{Ca,L}$-triggered Ca^{2+}-transient (CaT) and whole-cell caffeine-triggered Ca^{2+}-transient (cCaT; bottom). Inset: transverse line-scan representation of [Ca^{2+}]$_i$ at center of virtual cell, showing Ca^{2+}-wave propagation from subsarcolemma to cell-center; color-scale below. **C.** Comparison between key Ca^{2+}-handling properties in the model (Mdl, black bars) compared to experimental data in Ctl myocytes (Exp, white bars, from Figures 2,4,6). Top left: peak $I_{Ca,L}$-amplitude, Top middle: CaT-amplitude, Top right: time-constants of CaT-decay, Bottom left: SR Ca^{2+}-leak, Bottom middle: SR Ca^{2+}-load (amplitude of cCaT), Bottom right: time-constants of cCaT-decay.

Numbers indicate myocytes/patients (for experimental data). Experimental data are shown as mean±SEM; model simulations produce single value (no error-bar relevant).

Figure 8.
Computational analysis of SR Ca^{2+}-leak and spontaneous Ca^{2+}-release events (SCaEs). **A.** Voltage-clamp protocol and transverse line-scan representation of $[Ca^{2+}]_i$ at center of virtual cell in the Ctl model, Ctl model with increased SR Ca^{2+}-uptake, Ctl model with RyR2 dysregulation and pAF model combining both elements (top to bottom). The protocol shows the two final depolarization-triggered Ca^{2+}-transients at steady state, followed by a quiescent period to assess SCaEs, and simulated application of tetracaine and caffeine to determine SR Ca^{2+}-leak and SR Ca^{2+}-load. **B.** Quantification of incidence (top) and average amplitude (middle) of SCaEs. Bottom panel shows amplitude of SCaE-induced membrane currents. Results are presented as relative changes versus Ctl for increased SR Ca^{2+}-uptake (↑Serca2a), RyR2-dysregulation (↑RyR2), and pAF models. **C.** Similar to panel B for SR Ca^{2+}-load (top) and SR Ca^{2+}-leak (bottom).